



LAWRENCE
LIVERMORE
NATIONAL
LABORATORY

Light Output and Thermal Blast Analysis of Nuclear Fireballs

A.C. Delmastro, G.D. Spriggs

December 20, 2018

Film Rescanning and Re-Analysis Project Progress Report

Disclaimer

This document was prepared as an account of work sponsored by an agency of the United States Government. Neither the United States Government nor Lawrence Livermore National Security, LLC, nor any of their employees, makes any warranty, express or implied, or assumes any legal liability or responsibility for the accuracy, completeness, or usefulness of any information, apparatus, product, or process disclosed, or represents that its use would not infringe privately owned rights. Reference herein to any specific commercial product, process, or service by trade name, trademark, manufacturer, or otherwise, does not necessarily constitute or imply its endorsement, recommendation, or favoring by the United States Government or Lawrence Livermore National Security, LLC. The views and opinions of authors expressed herein do not necessarily state or reflect those of the United States Government or the Lawrence Livermore National Security, LLC, and shall not be used for advertising or product endorsement purposes.

Auspices Statement

This work was performed under the auspices of the U.S. Department of Energy by Lawrence Livermore National Laboratory under Contract **DE-AC52-07NA27344**

I. Introduction

During the 1940s, 50s, and 60s, there were 210 atmospheric nuclear tests. Every test was extensively recorded with high quality motion picture films and photographs, providing a unique historic record, containing ~10,000 films, with a total of ~22 million frames of information. Much of what is known about the effects of nuclear weapons has been obtained from these tests. There are approximately 6500 scientific films that are in the process of being scanned by Lawrence Livermore National Laboratory and re-analyzed using modern computer techniques.

The four major effects of a nuclear detonation are prompt radiation, shockwave, thermal blast, and fallout.

Thermal blast is a measure of the instantaneous heat loss rate from the fireball. The light output from a detonation represents the fraction of the thermal pulse that occurs in the visible light range. For near-surface detonations, two distinct light pulses are produced:

- The 1st pulse is produced by the formation and subsequent cooling of the shockwave
- The 2nd pulse is produced by the change in the opacity of the shockwave front and the subsequent cooling of the hot gases left behind in the fireball

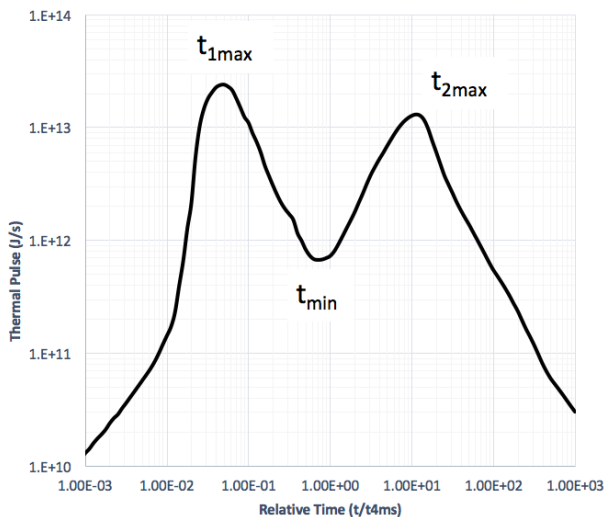


Figure 1: Example of a power pulse vs. time plot, with the key components of a thermal pulse curve: t_{1max} , t_{min} , and t_{2max} .

The three key times of the double pulse are at t_{1max} , t_{min} , and t_{2max} . These light pulses are used by the military to monitor foreign nuclear tests and calculate the yield of such detonations.

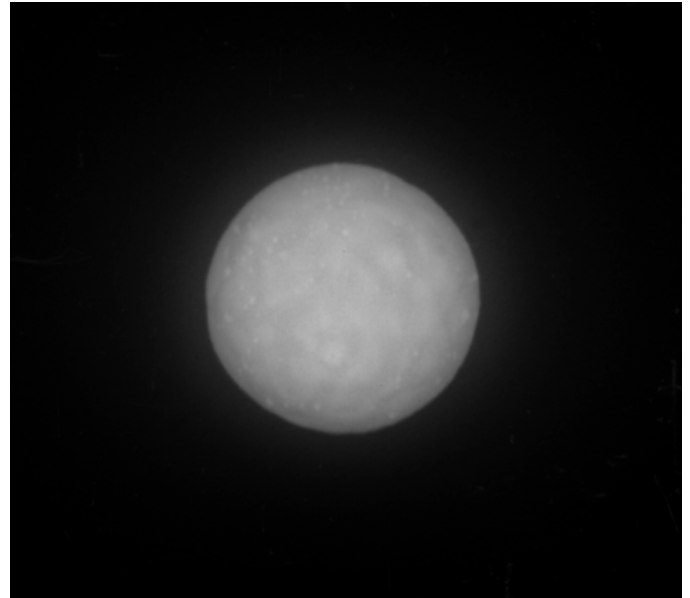


Image 1: Frame 174, Wasp Prime Film 29302 at t_{min}

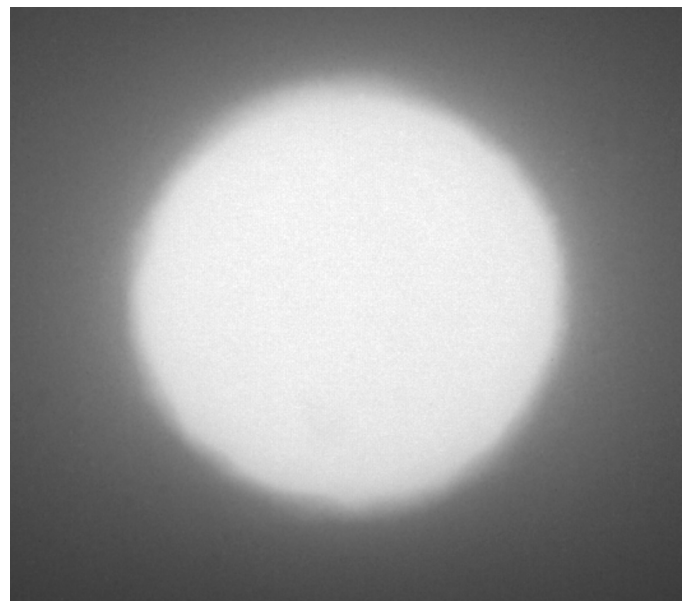
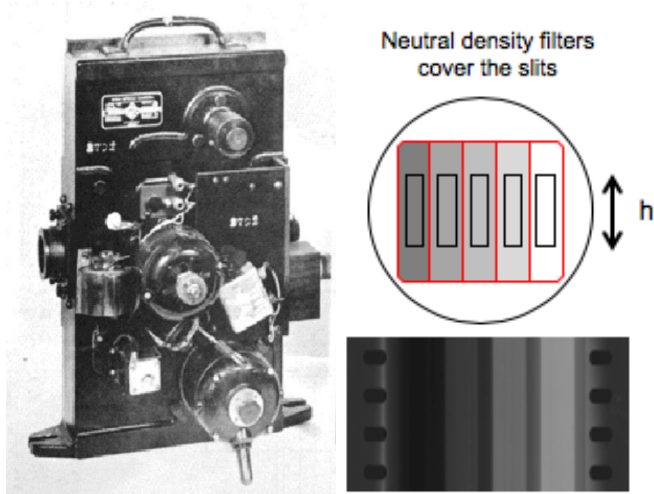


Image 2: Frame 288, Wasp Prime Film 29302 at t_{2max}

The thermal pulse from a nuclear detonation is very complicated and goes through several distinct heat transfer phases. Analyzing each of these heat transfer phases can provide us with basic information concerning thermal blast phenomenon.

Nuclear fireballs act as blackbody radiators. Their light output is dependent on their thermal radiation and emissive power.

Streak cameras were used to capture a very detailed history of the light output from a nuclear detonation. These types of cameras were more useful than the rotating prism cameras (i.e., fireball cameras) since they ran continuously, leaving no gaps in the data. Since the first pulse is very short-lived, fireball cameras frequently missed the beginning of the first pulse, despite running at ~3000 frames per second. In addition, recording frame-by-frame leaves gaps in the light recording.



Images 3-5: General Radio (GR) Slit camera; Layout of descending neutral density (ND) filters; Example streak frame with 4 streaks

Streak cameras had neither shutters or lenses (in most cases); the film moved continuously behind the slits. Neutral density filters (and, occasionally, color filters) of various optical densities were placed over the slits to control the amount of light striking the film, which minimized the probability of saturating all of the streaks captured on the film. Other combinations of color filters and/or film emulsions could be used to collect spectra data. Using these streak cameras, the light-output signature from a detonation could be easily measured. And, from these signatures, key times associated with each of the two pulses

could be correlated with the yield of the detonation.

Unfortunately, extracting the data from these types of films was easier said than done. Based on the relatively crude techniques that were available back in the 50's and 60's, the streak films were rarely analyzed. Consequently, for the last 50 years, the military has been using correlations developed from other types of instrumentation, such as bhangmeters and calorimeters, to describe the characteristics of a thermal pulse. Although these correlations are adequate for most military applications, more precise correlations are needed to validate modern computer codes, such as HYCHEM, that attempt to simulate nuclear effects.

II. Research Objectives

The objective of this interim report is to describe recent efforts to extract benchmark data from the existing streak films using modern Figure-processing techniques. These new and, hopefully, greatly-improved data will provide our code developers with the benchmark data necessary to validate our modern computer codes that simulate nuclear weapon effects.

III. Methodology

There are ~85 streak films representing 27 shots.¹ All streak films were rescanned using various "Look-Up Tables" (LUTs) calibrated to each particular film stock. Step wedges at the beginning of each film provided a range of optical density vs. exposures used to generate these LUTs. These LUTs were then used to ensure that the optical density at each point along the length of the film captured during the scan was an exact copy of the original film.

Once the films were scanned, a python code, developed by Aaron Kawahara, determined the average pixel intensity per row of pixels per streak. These pixel intensity values

¹ As of December 2018, it was discovered that there are ~20 other streak films at LANL to be analyzed.

were then converted to optical density. The amount of noise of the raw data was dependent on the film stock. Streak films recorded on MF film stock produced very low-noise data since it is a very fine-grained film, while streak films recorded on SXX film stock produced very noisy data since it is a much grainier film.

Smoothing algorithms were implemented to reduce the amount of noise that was observed over the length of the film.

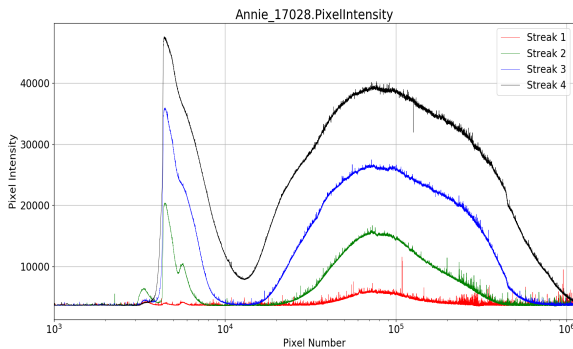


Figure 2: Pixel Intensity plot for Annie_17023 (MF stock)

The absolute time at each point along the length of the film was found by measuring the instantaneous frame rate over the length of the film and converting these data to a *time-per-pixel*. The frame rate was measured using a custom tool developed at LLNL that measures the location of each timing mark in the perforation area of the film.

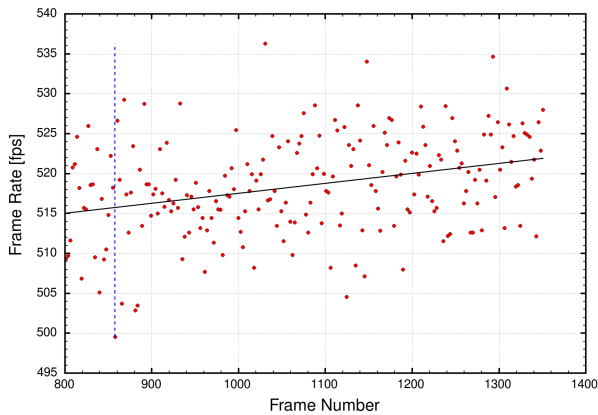


Figure 3: Example of a frame rate plot

As it turns out, many of the streak films had a relatively constant, or slowly increasing, frame rate. In these cases, a simple polynomial fit was used to approximate the frame rate as a function of absolute frame number (seen in figure 3). In some cases, however, the timing

marks showed a somewhat erratic pattern. An example of this is shown in figure 4. It is believed that this erratic behavior is due to slippage of the motor belt. For these cases, the absolute time was determined using the instantaneous frame rates as inferred from the timing marks.

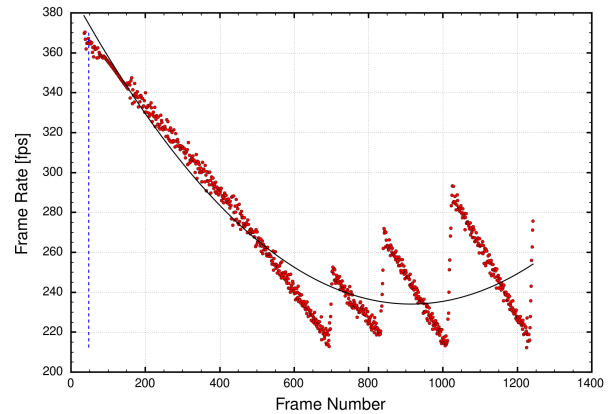


Figure 4: Example of frame rate plot in which the frame rate changes very rapidly

In order to calculate the absolute time, two Fortran subroutines were developed, Get_POFL and Get_Time. The former finds the pixel of first light (POFL) by taking the average of the base of each streak and then determines at which point the intensity increases by a certain threshold. Then, the latter subroutine finds the frame rate at each pixel, takes the inverse, and then integrates the time difference between subsequent pixels to find the absolute time at each pixel.

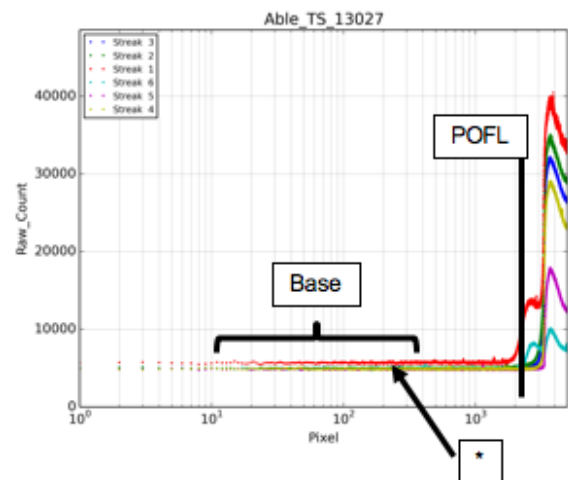


Figure 5: Demonstration of first 1000 pixels before POFL

Though these shots were conducted in the early morning, when there was sunlight, the base of the film was exposed, which would then

be corrected before analysis. In addition, frequently, there would be a “light leak” before the brightest pixel on the right and left sides of the film. This, therefore, makes calculating POFL more complicated. The POFL was then taken from the less bright streaks (lane 3 or 4).

The thermal fraction, f , shown in the above equation was determined by taking a weighted average of the frequency bands in the visible light spectrum as predicted by HYCHEM. This allowed us to compare the data from the streak cameras to the predictions by HYCHEM.

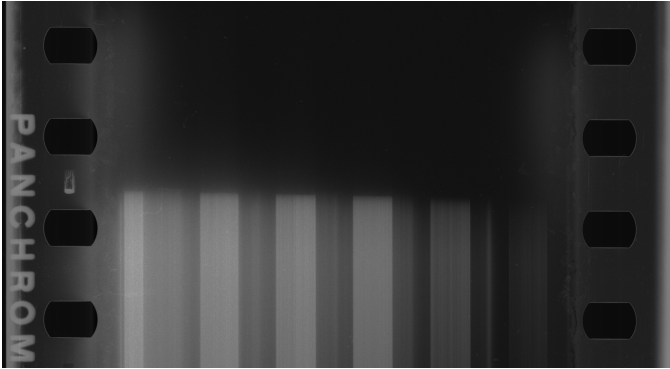


Image 6: Frame of POFL and demonstration of “light leaks” on both sides of the frame

Hurter-Driffield (HD) curves were developed using step wedges from films of each emulsion and color filter combination. These HD curves are used to convert optical density to exposure, utilizing linear interpolation.

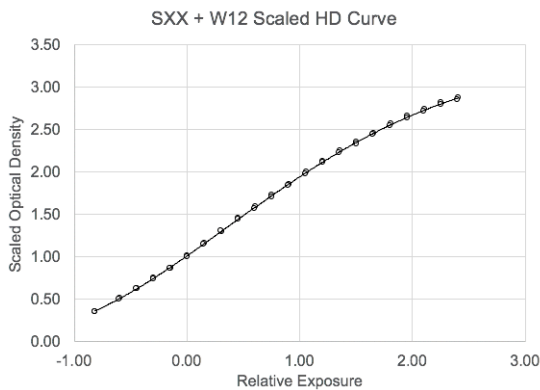


Figure 6: HD Curves for SXX+W12 emulsion/color filter combination

The thermal power was calculated from the corrected exposure data via,

$$P(t) = E(t) \cdot \frac{fY}{\sum_i E_i \Delta t} \quad (1)$$

Since the exact thermal fraction for a particular detonation is not usually known, the streak camera data was normalized such that the area under the total light-output curve is equal to 1.0.

IV. Streak Film Preliminary Results

TIME-DEPENDENT EXPOSURE CURVES

If the HD curve for each film stock is sufficiently accurate, all of the streaks on any given film should overlap with each other when normalized to the same point in time. An example of this is shown in Figure 7. In order to obtain an accurate HD curve for each film, the gamma for that particular film had to be measured. This was accomplished by noting the change in optical density going from one streak to another streak at the same point in time. Once it was shown that the streaks overlapped, an average value was then calculated using all of the applicable streaks (see Figure 8).

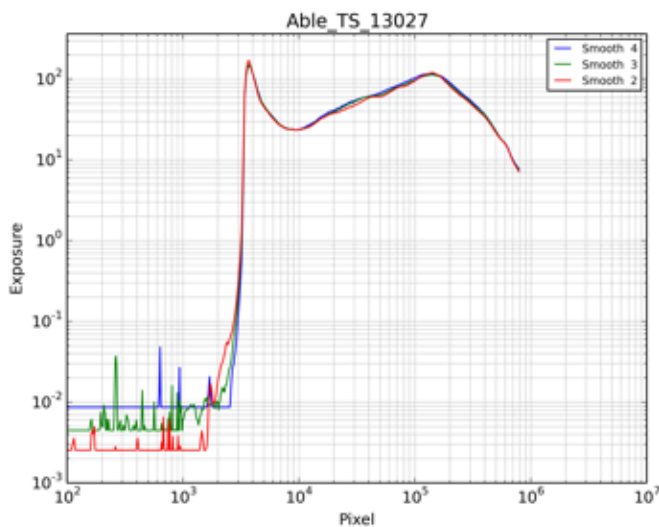
Comparisons between films of the same shot are given with Figures 9 & 10 for the Baker_BJ shot and Figures 11-13 for the Sugar shot. In both Baker_BJ films, 10651 and 10654, the streaks overlapped with each other when normalized. Despite being normalized, the exposure magnitudes differ by a factor of 4-5. This is assumed to be caused by the fact that these films have different emulsion/color filter combinations. Regarding the Sugar films, 11011 and 11012 (Figures 11 and 12, respectively) share exposure values in the same magnitude, probably due to the fact that they both were on MF stock. In addition, it is assumed that the magnitude of these two films and 11033 (Figure 13) differ by a factor of 4 because 11033 has an SXX emulsion.

The shape of double pulses of the two airdrops (Able_TS and Baker_BJ) are significantly different to that of surface shot, Sugar, which indicates that there is a dependence between the shape of the double pulse and the type of shot. The peak of the first pulse is significantly higher in magnitude compared to that of the second pulse for surface shots; however, for airdrops, it appears that the magnitudes of the peaks from the first and second pulses are very similar.

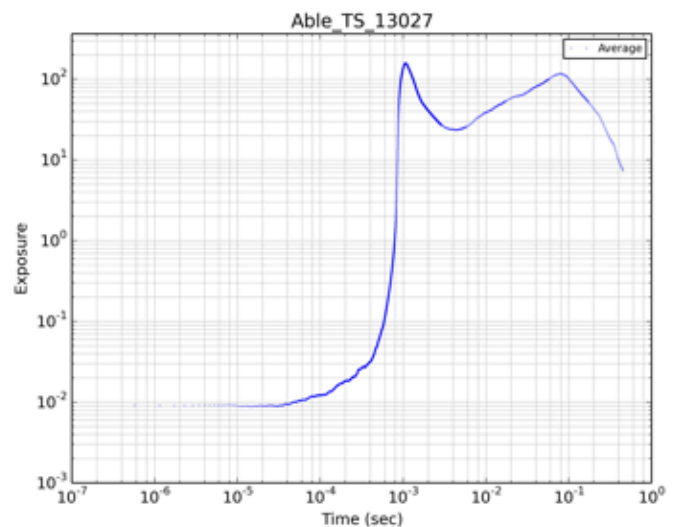
*Note: The noise before the first pulse is negligible noise from the base of the film (Exposure axis in logarithmic scale).

Able TS – AirDrop Shot Example:

Normalized Exposure Curves

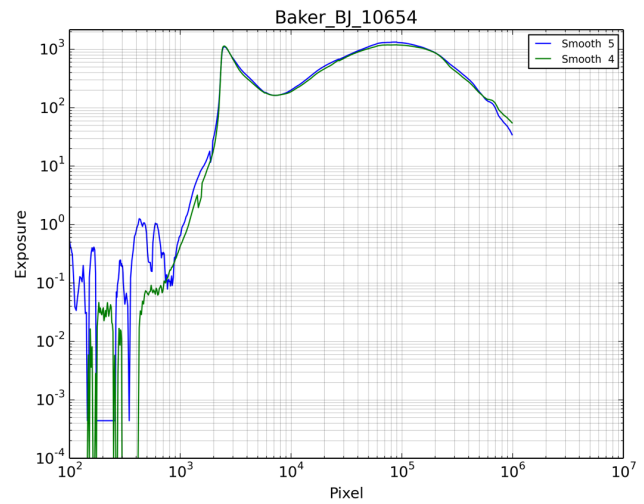
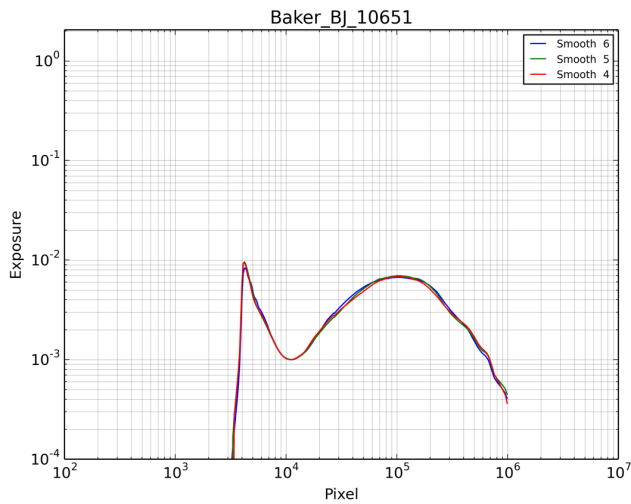


Average Exposure over Time



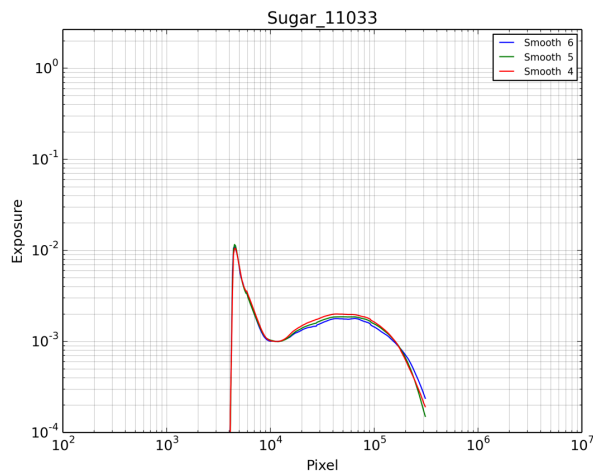
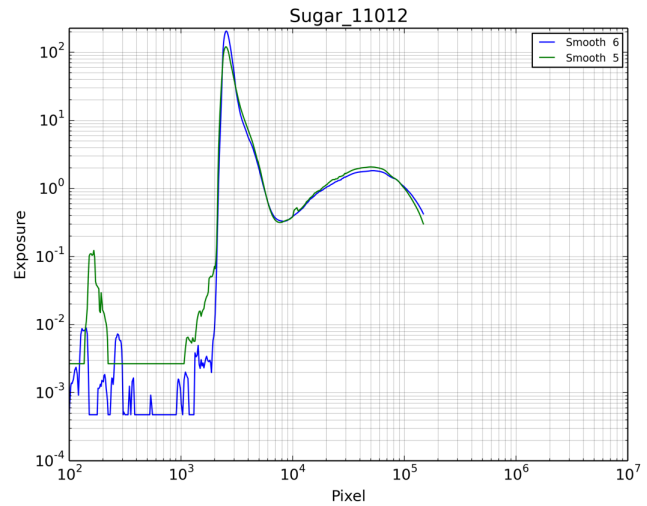
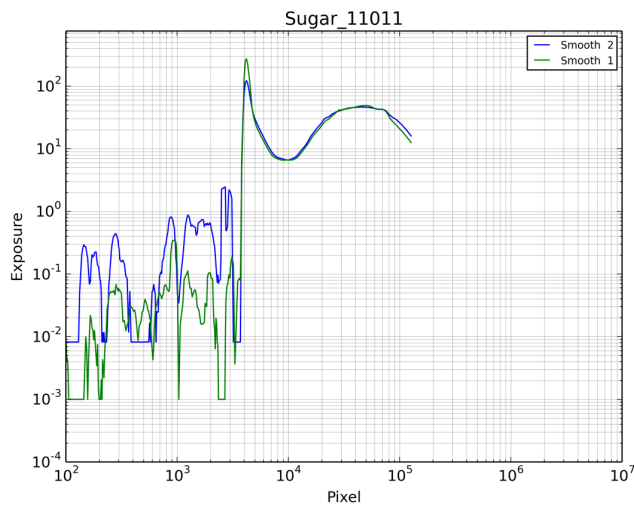
Figures 7 & 8: Normalized exposure vs. pixel of Able_TS_13027 film for streaks 2,3, and 4 (SXX W12); Average exposure vs. absolute time of Able_TS_13027 film for streaks 2,3, and 4.

Baker BJ – AirDrop Shot Example:



Figures 9 & 10: Normalized exposure vs. pixel of Baker_BJ_10651 film for streaks 4,5, and 6 (SXX W47); Normalized exposure vs. pixel of Baker_BJ_10654 for streaks 4 and 5 (SXX W12)

Sugar – Surface Shot Example:



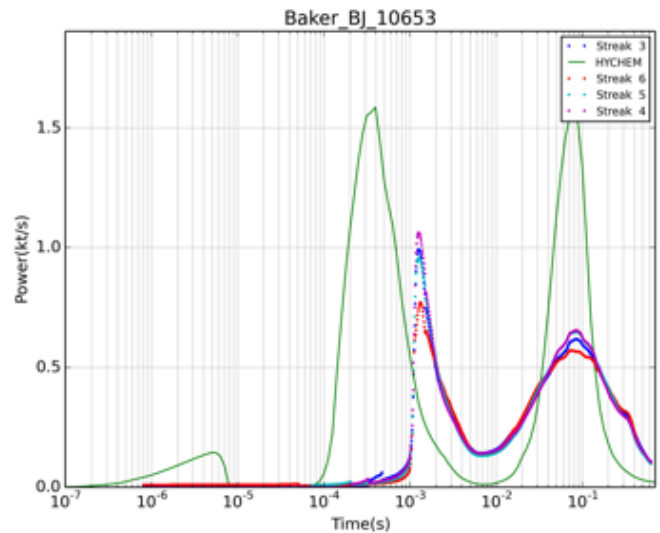
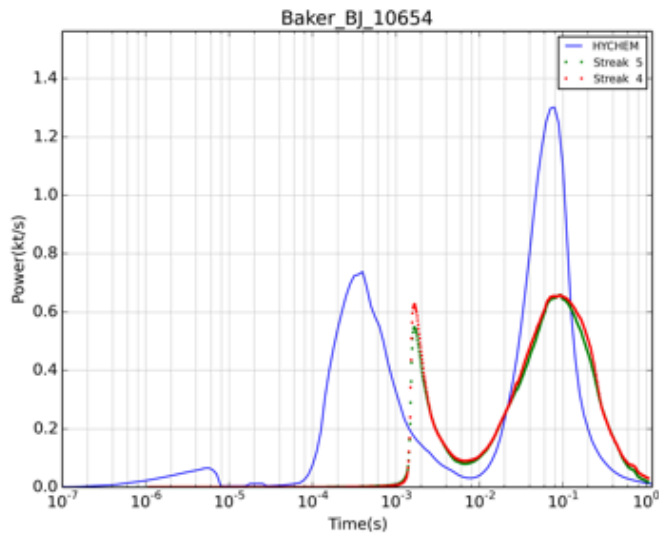
Figures 11 - 13: Normalized exposure vs. pixel of Sugar_11011 film for streaks 1 and 2 (MF W29); Normalized exposure vs. pixel of Sugar_11012 for streaks 5 and 6 (MF no Filter); Normalized exposure vs. pixel of Sugar_11033 film for streaks 4,5, and 6 (SXX W47)

POWER COMPARISON BETWEEN FILTERS OF SAME SHOT

After properly normalizing the streak data, the data can be directly compared to HYCHEM's prediction (see Figures 14 and 15). As can be seen, the magnitude of the first peak is significantly impacted by the choice of color filter (i.e., W12 vs. W47). The film data magnitudes are notably less than those of HYCHEM's prediction. This discrepancy needs to be resolved. In addition, the film data appears to be shifted in time compared to HYCHEM's solution; this disparity will be analyzed in the following section.

SXX W12 Filter

SXX W47 Filter



Figures 14 & 15: Power vs. time of Baker_BJ_10654 film for streaks 4 and 5 (SXX W12); Power vs. time of Baker_BJ_10653 film for streaks 4,5, and 6 (SXX W47)

HYCHEM AND FILM DATA COMPARISON OF LOW YIELD SHOTS

One area of interest is to see how the shape of the double pulse is affected with changing yield. In preliminary analysis of the shape of Ray, which has a yield of 0.38 kt, from the streak film 17428, there is only one distinct pulse with a small bump a few thousand pixels after t_{1max} . Despite the fact that Figure 16 is not converted to thermal power, the difference in shape between HYCHEM's prediction and the film's light output measurement demonstrates that HYCHEM may not be accurately representing the shape of the double pulse at low yields.

This discrepancy will be further analyzed once the film analysis has been finalized for shots Ray and Ruth, both of which with yield less than 0.5 kt.

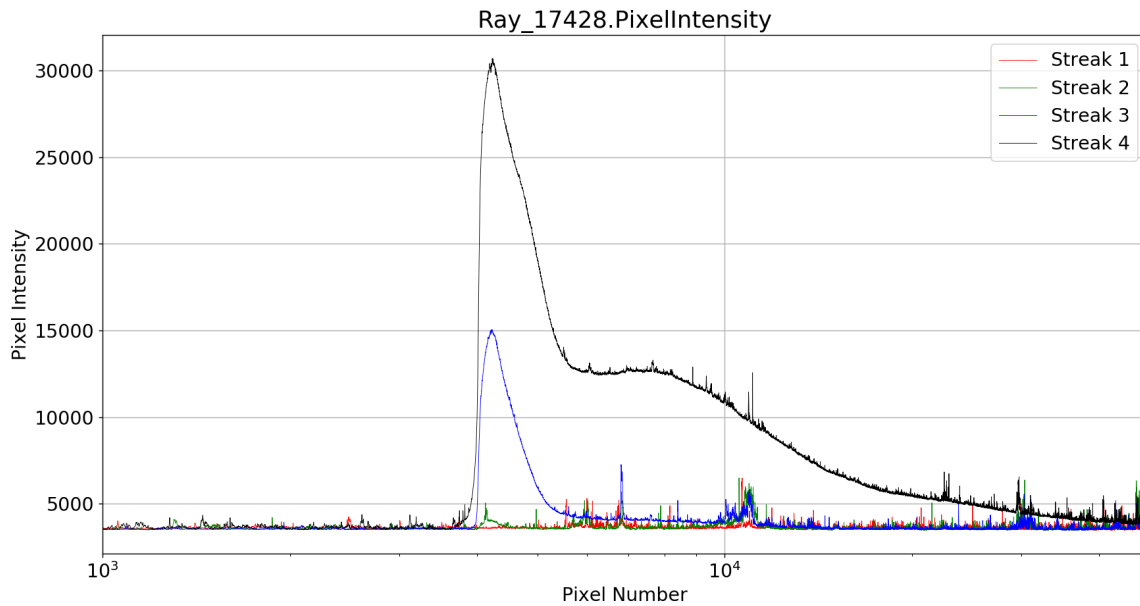


Figure 16: Pixel intensity vs. pixel number of Ray_17428

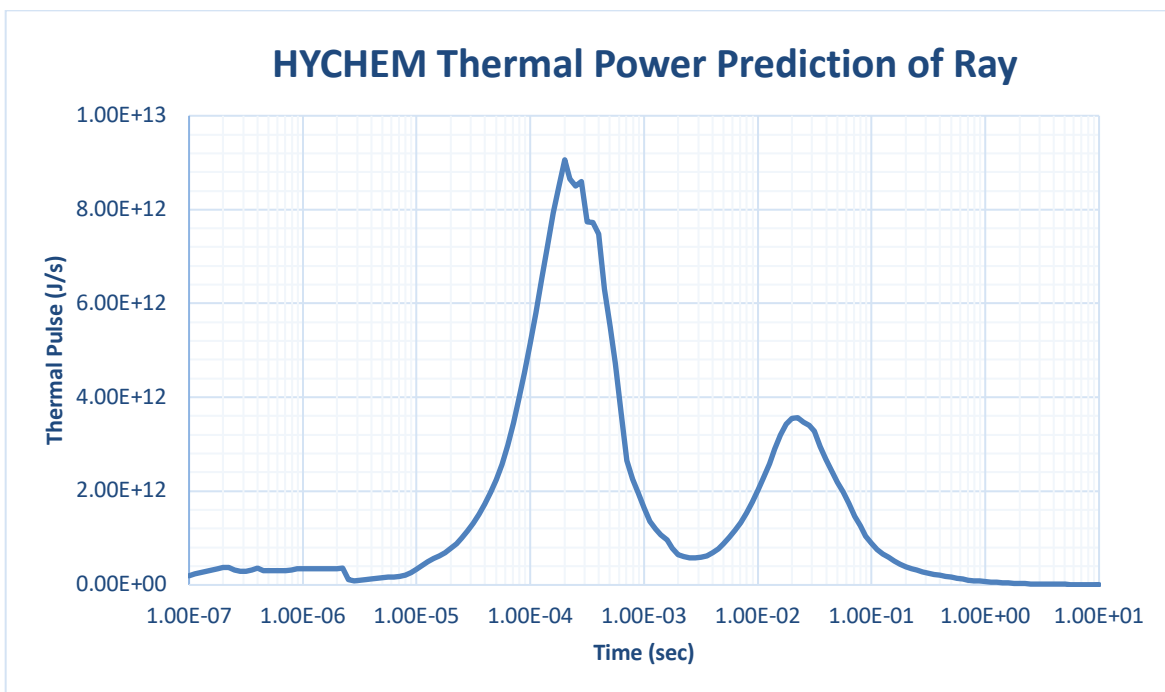


Figure 17: Thermal power vs. time of HYCHEM simulation of Ray shot (yield: 0.38 kt)

DIFFICULTIES CHOOSING POFL

Selecting the POFL has not very simple despite the fact that frame of first light is very discernable. Each pixel represents ~1 microsecond; therefore, if the POFL is off by 400 pixels, the plot becomes shifted by almost one millisecond. This is a significant amount of time since one goal is to use this data to develop new correlations at each of the key times. The t_{1max} occurs in the decimilli- and millisecond range; therefore, an offset of 100 pixels can lead to an error of ~25%, depending on the yield. For this reason, further research is necessary in order to find the exact POFL and minimize error on the time.

For the figures below, three different POFL were selected. The accuracy of the POFL was determined by how close the t_{min} value was with respect to that estimated from the t_{min} correlation^[3]:

$$t_{min} = 0.0039 \left(\frac{\theta Y}{\rho} \right)^{0.433} \tag{2}$$

As a result, figure 18 (A) had the closest t_{min} with respect to that of the correlation (12.2 ms vs. 11.8 ms, respectively). Despite the fact that this POFL had the closest t_{min} value, there was still a significant shift compared to the HYCHEM prediction. This difference will be further investigated as it is unknown whether HYCHEM is accurate at these early times.

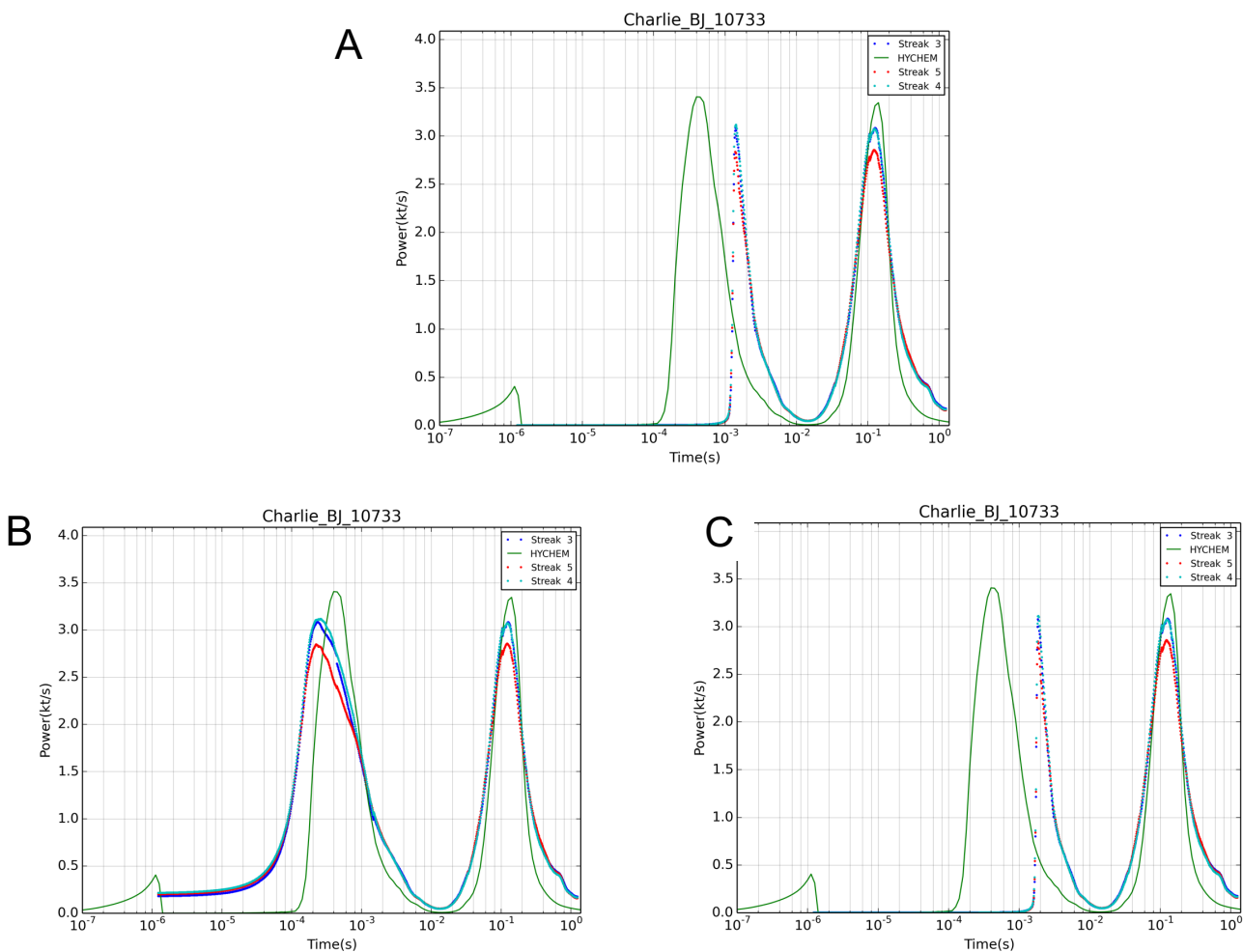


Figure 18: Power vs. time plots of Charlie_BJ_10733: A) POFL – 1617; B) POFL – 2573; C) POFL – 1241

V. Original HYCHEM Results (2017)

In 2017, a parametric study of the light output vs. time was performed using HYCHEM. During this study, we sought to answer two questions: 1) how does the shape of the double pulse change as a function of air density, and 2) how does the shape of the double pulse vary with increasing mass/yield ratio. The latter study also examined how the shape of the double pulse from various mass/yield ratios changed with decreasing air density. Both studies analyzed simulations with a yield of 1 kt.

HYCHEM predicted that the power at t_{\min} and $t_{2\max}$ increases as the air density decreases. The time at t_{\min} appears to be weakly dependent on air density, whereas $t_{2\max}$ shifts dramatically. In addition, as the air density decreases (i.e. as the altitude of the detonation increases), the double pulse starts to disappear. For this 1 kt and 10 kg/kt shot, the double pulse merges to form a single pulse at ~ 0.005 kg/m³, within the Stratosphere.

AIR DENSITY PARAMETRIC STUDY

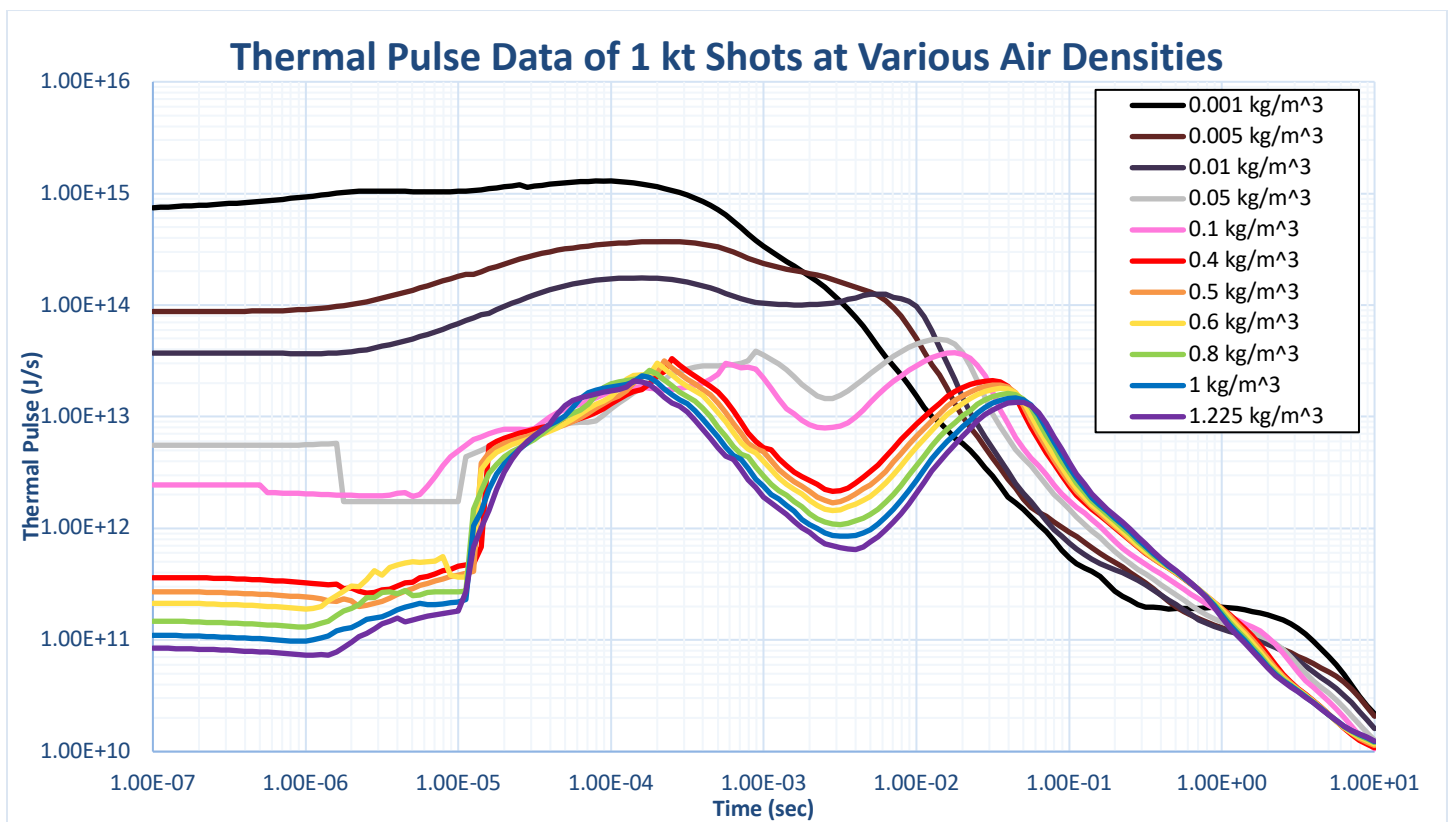


Figure 19: Thermal pulse vs. air density for a 1 kt detonation (10 kg/kt)

MASS/YIELD PARAMETRIC STUDY

At high air densities, the mass/yield ratio demonstrates a very minimal effect on the power of the second pulse, specifically at t_{\min} and $t_{2\max}$; the curves overlapped on the second pulse at these higher air densities. Once the air density decreases below 0.25 kg/m^3 , at which point the nuclear detonation would be within the Stratosphere, there was a noticeable distinction between the power curves. In addition, the double pulse started to disappear. At 0.01 kg/m^3 , both pulses were apparent with shots of 1 kg/kt and 10 kg/kt . At the lower ratios, $t_{2\max}$ disappeared, whereas, at higher ratios, $t_{1\max}$ would disappear. At 0.001 kg/m^3 , the two pulses merged into one single pulse. The curves at very early times are not relevant to the double pulse; the data regarding heat transfer at such early times is limited. For the plots with air densities below 0.1 kg/m^3 , they demonstrated that the $P_{2\max}$ for the 1000 kg/kt shot was much lower than that of the 100 kg/kt shot.

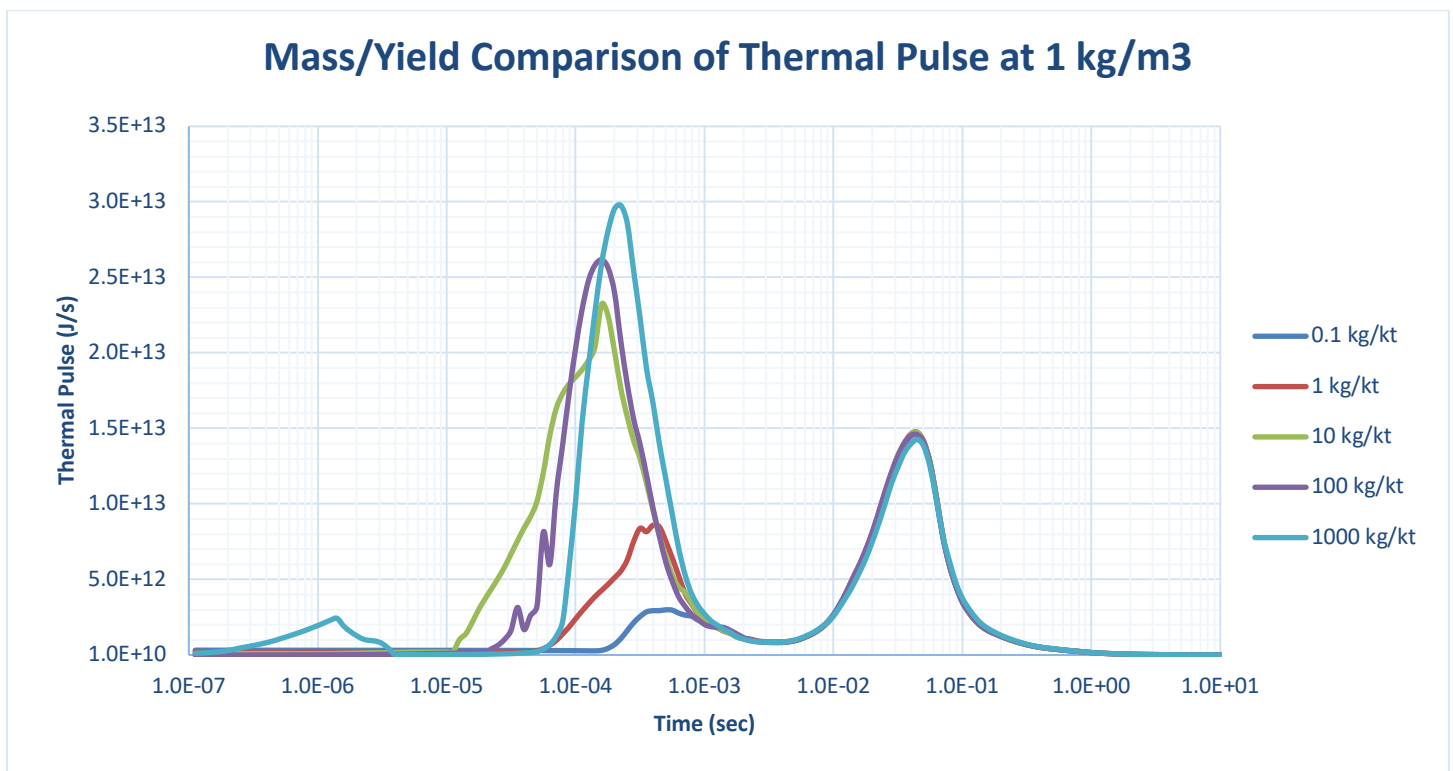


Figure 20: Comparison of 1 kt shots at an air density of 1 kg/m^3 with various mass/yield ratios

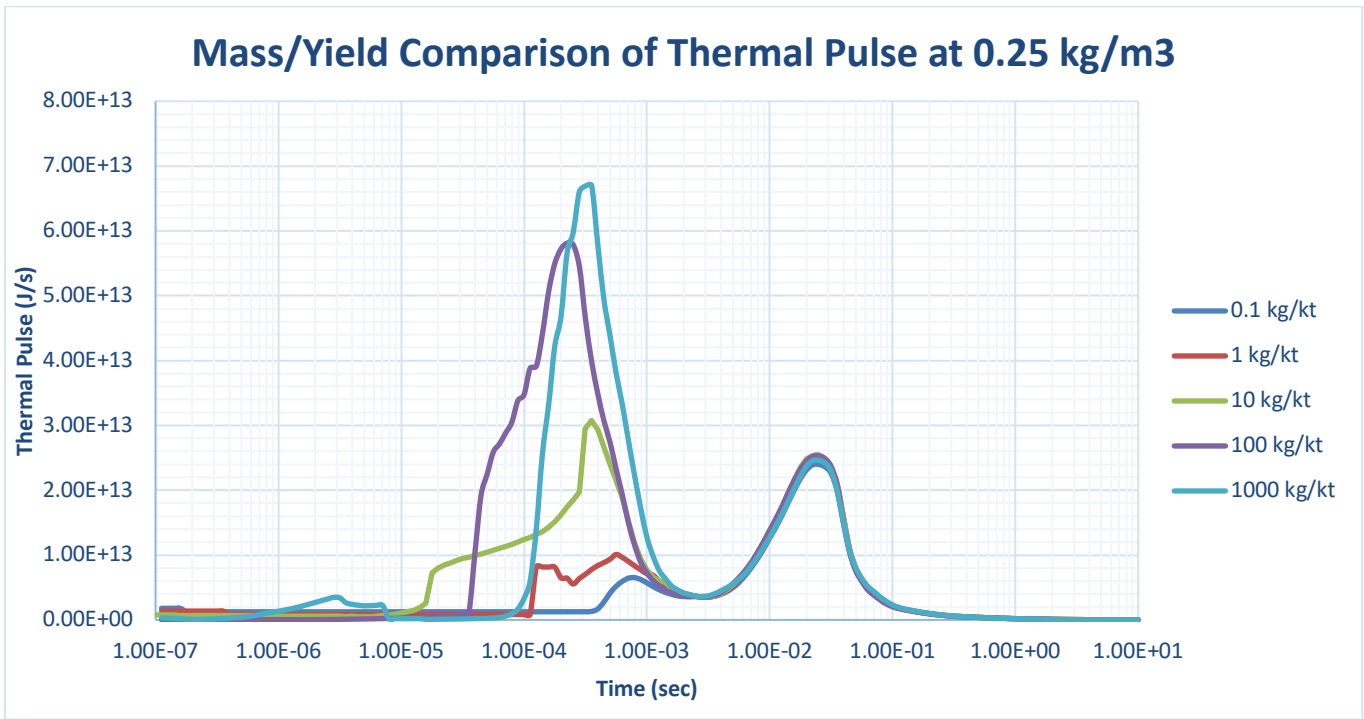


Figure 21: Comparison of 1 kt shots at an air density of 0.25 kg/m³ with various mass/yield ratios

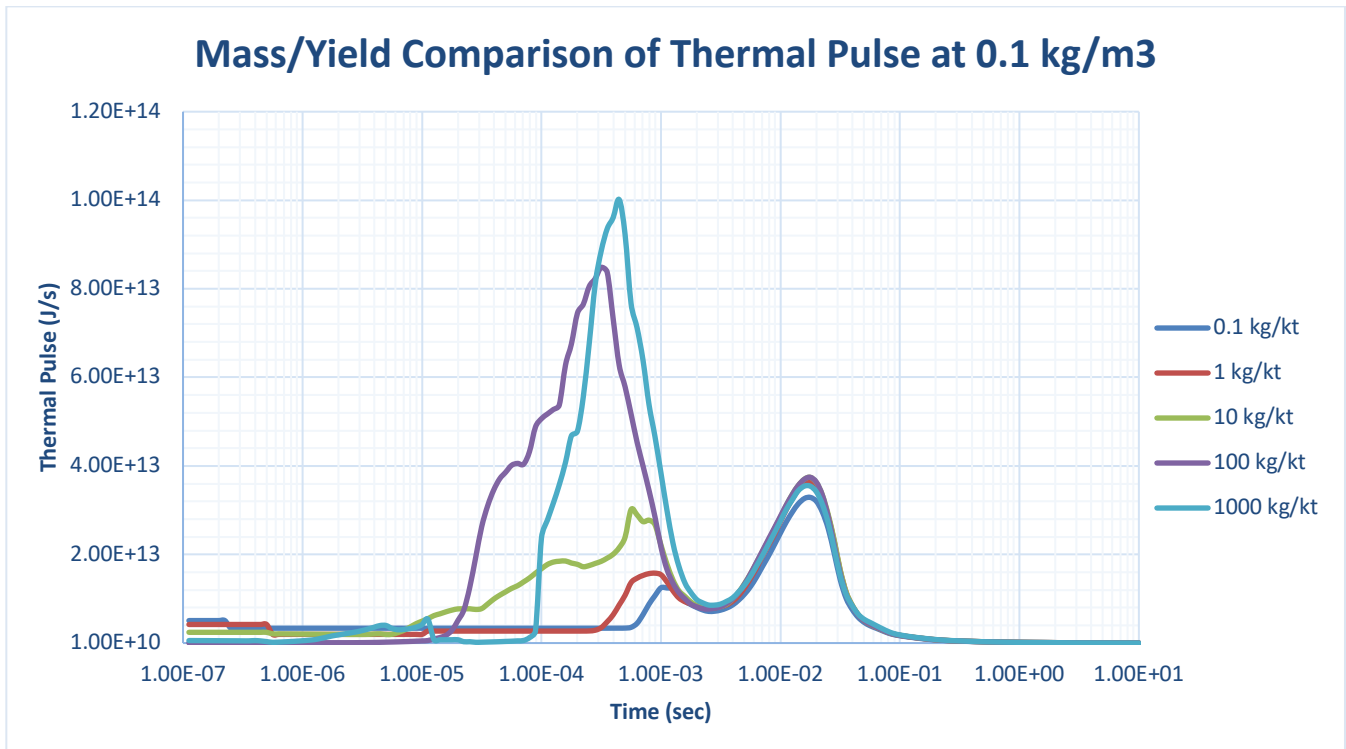


Figure 22: Comparison of 1 kt shots at an air density of 0.1 kg/m³ with various mass/yield ratios

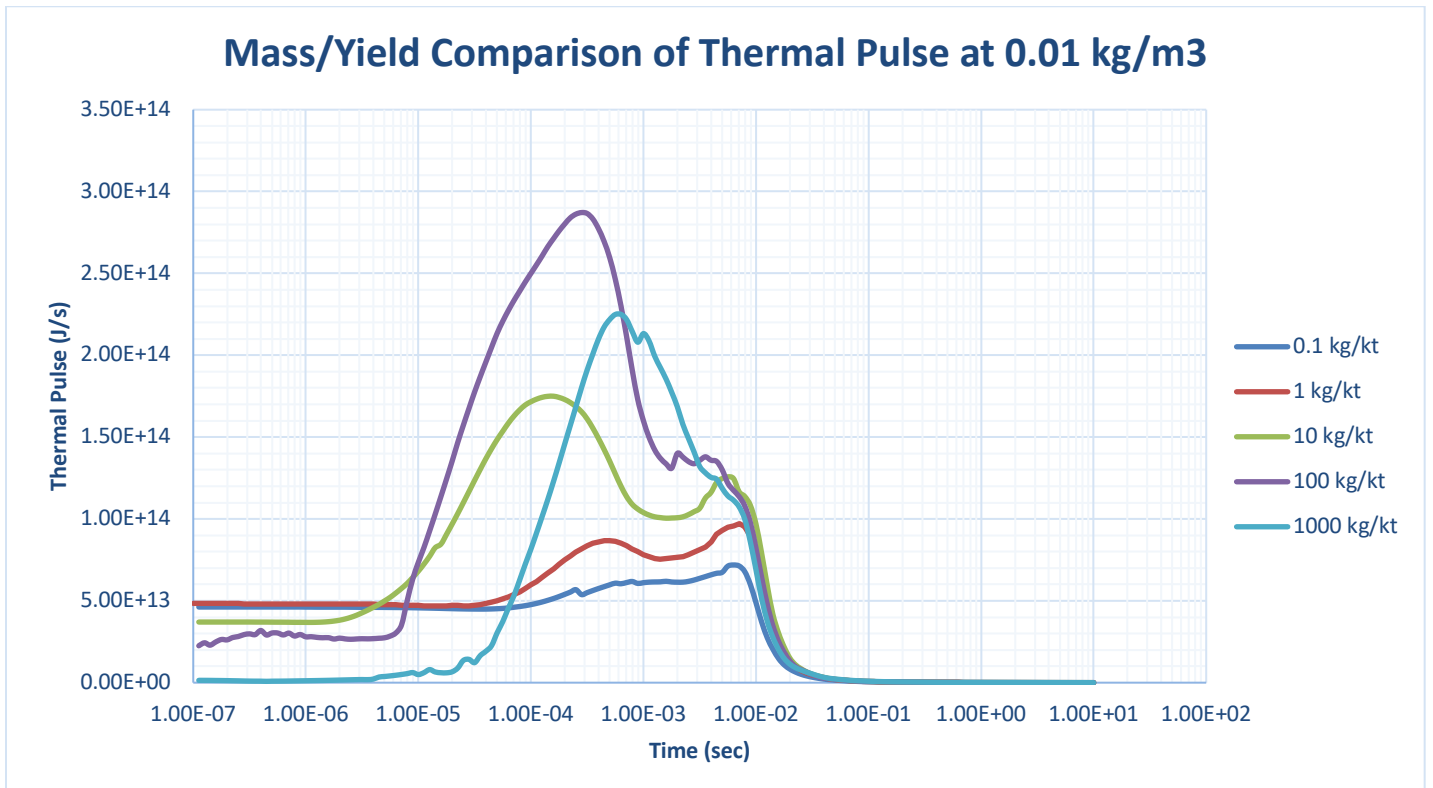


Figure 23: Comparison of 1 kt shots at an air density of 0.01 kg/m³ with various mass/yield ratios

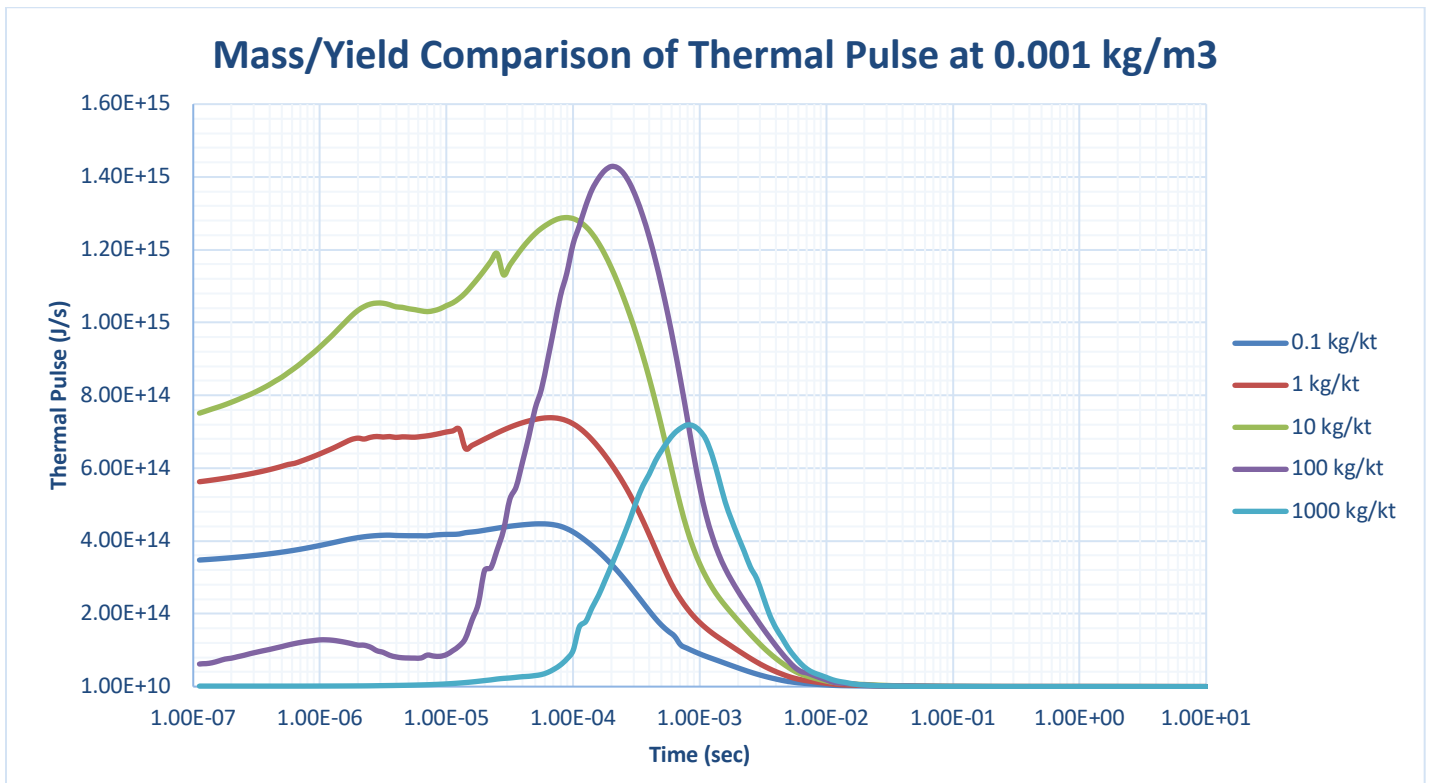


Figure 24: Comparison of 1 kt shots at an air density of 0.001 kg/m³ with various mass/yield ratios

HYCHEM CORRELATIONS

Note: an asterisk represents the curves that use data from shots of various yields and mass-to-yield ratios.

The mass/yield parametric study determined that at air densities within the Troposphere, mass/yield ratios have almost no effect on the key time or power parameters of the second pulse. In addition, based on the fact that t_{2max} , P_{min} , and P_{2max} change with air density, as demonstrated in figure 19, those results are analyzed more in-depth to develop mathematical correlations and determine reasonability of such conclusions.

○ Time Correlation

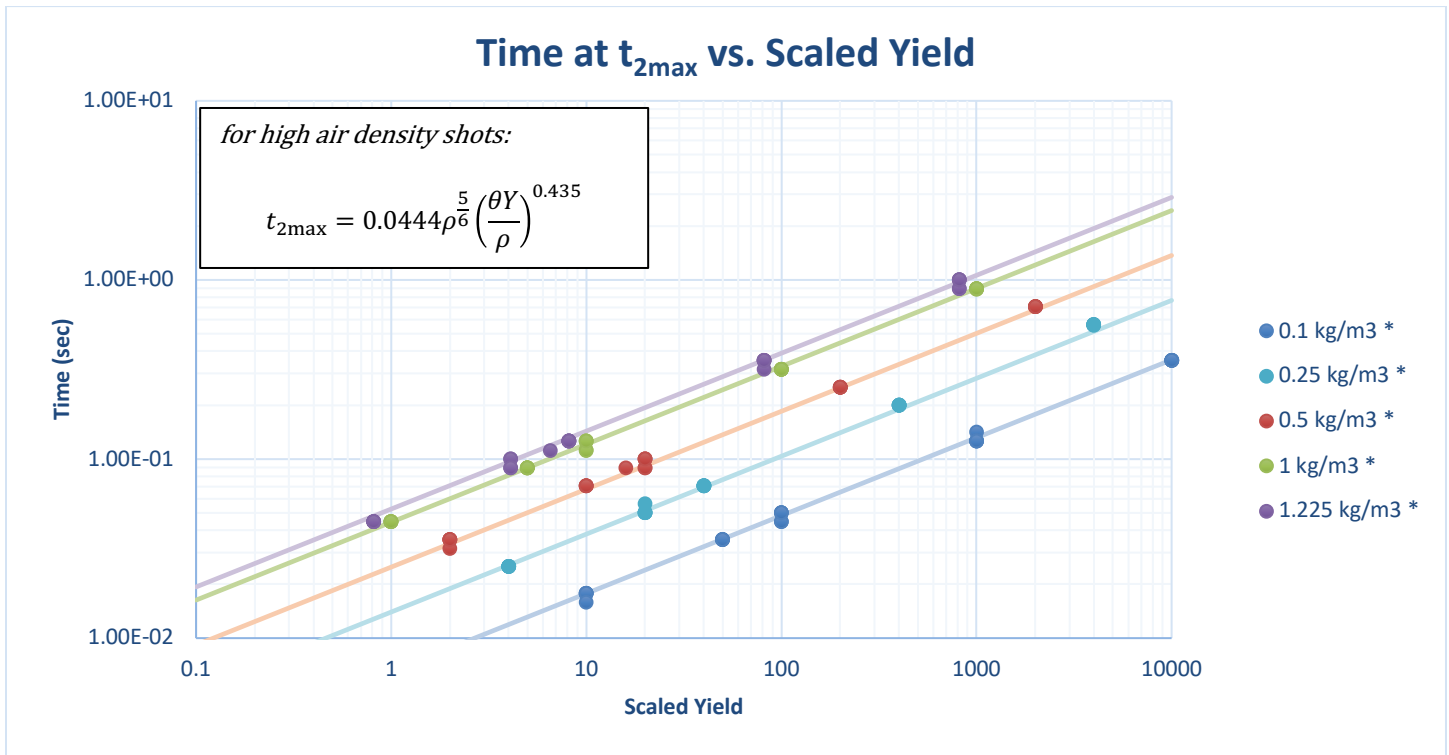


Figure 25: Comparison of time at t_{2max} vs. scaled yield using HYCHEM solutions

According to HYCHEM, t_{2max} is dependent on both the scaled yield as well as air density. As the air density decreases, the t_{2max} curve shifts downwards. It is apparent that the mass/yield ratio has little to no effect on t_{2max} .

	< 4.3 km	> 4.3 km
Northrup's approximation	$t_{2max} = 0.0417Y^{0.44}$	$t_{2max} = 0.0400Y^{0.45}\rho^{0.35}$
HYCHEM correlation	$t_{2max} = 0.0444\rho^{\frac{5}{6}}\left(\frac{\theta Y}{\rho}\right)^{0.435}$ (3) *for high air density shots	

Table 1: Comparison of previously used approximation for t_{2max} and newly developed power correlations using HYCHEM

Northrup's approximation for t_{2max} only considers air density for shots below 4.3 km. In the correlations derived from HYCHEM, equation (3), t_{2max} can be more accurately calculated as it considers the yield, type of shot (air drop or surface), and air density. This correlation can only be used at lower altitudes since low air densities lead to the disappearance of the double pulse, making it difficult to determine an accurate t_{2max} .

○ *Power Correlations*

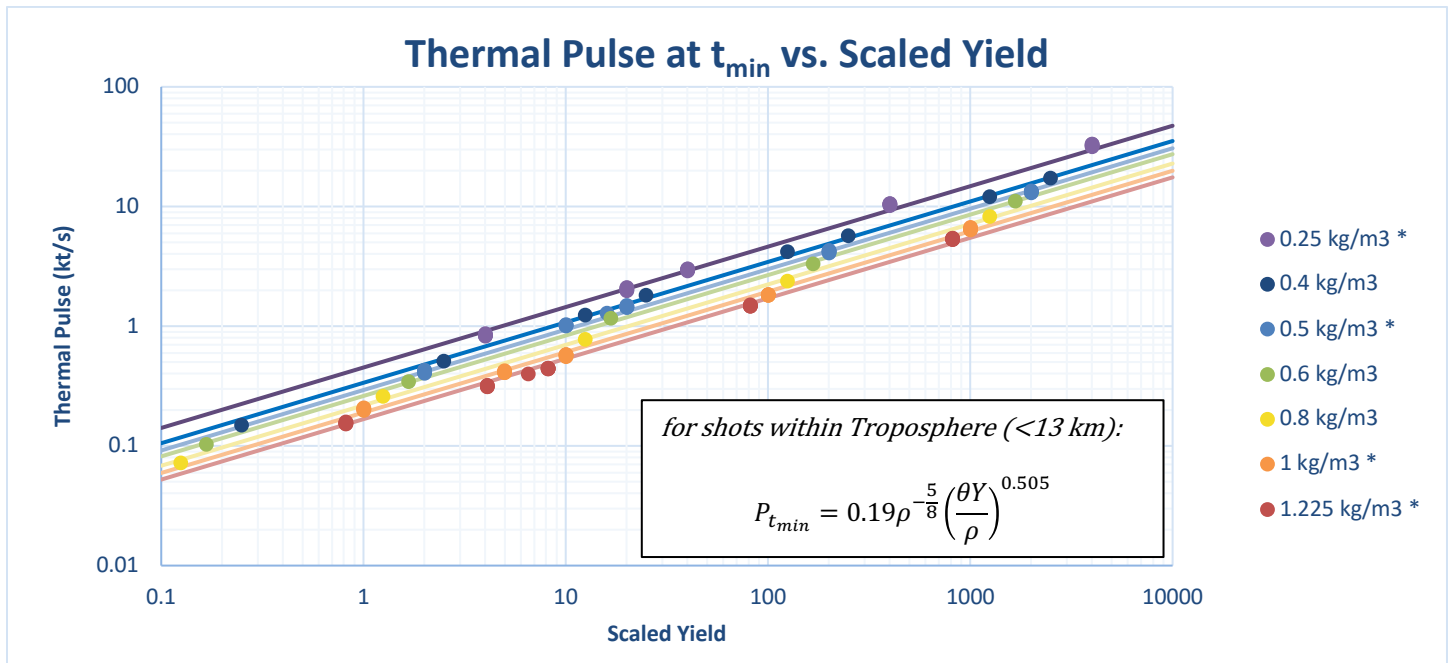


Figure 26: Comparison of thermal pulse at t_{min} vs. scaled yield (Equation 4)

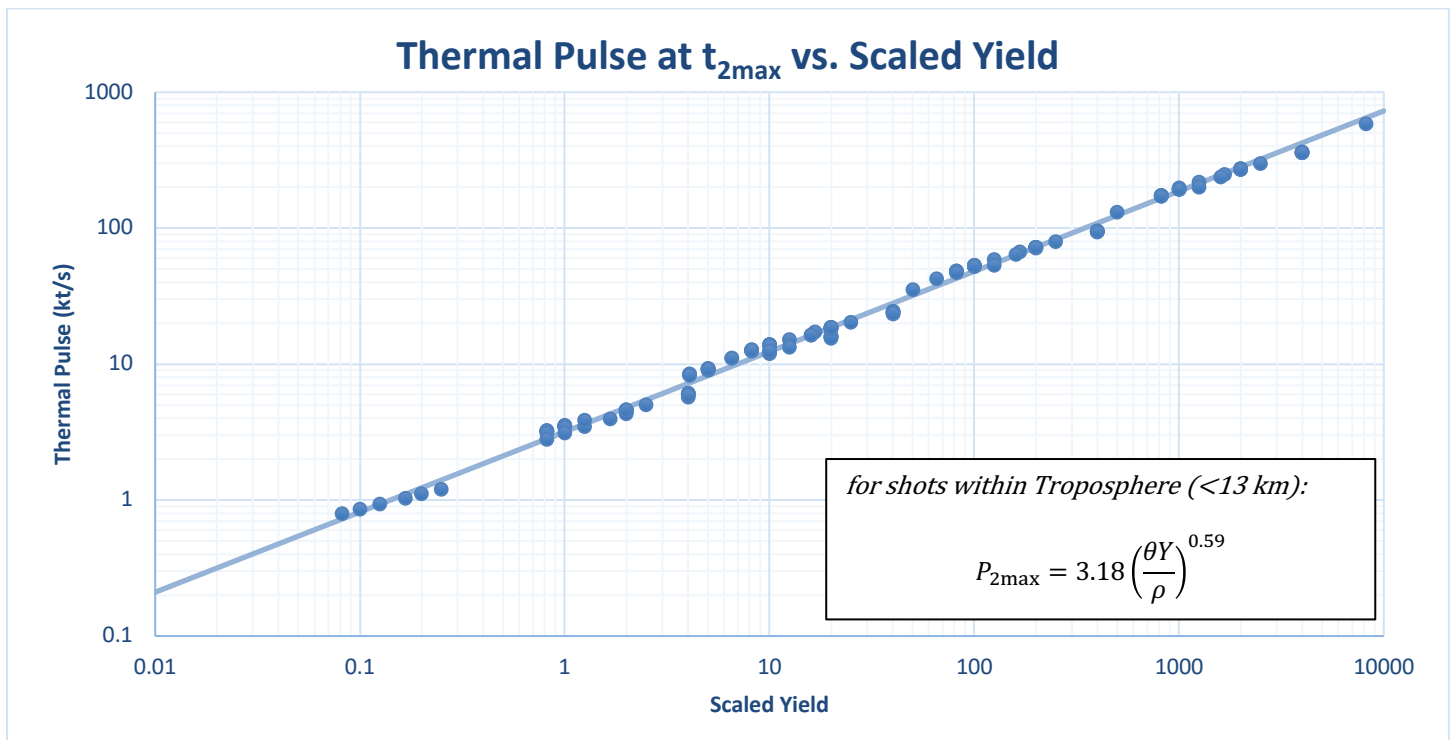


Figure 27: Comparison of thermal pulse at t_{2max} vs. scaled yield

For P_{min} , the curve shifts upwards as the air density decreases; on the contrary, the P_{2max} HYCHEM solutions all fall on one simple function in terms of scaled yield for all altitudes until the lower Stratosphere.

	< 4.3 km	> 4.3 km
Northrup's approximation	$P_{2max} = 3.18Y^{0.56}$	$P_{2max} = 3.1Y^{0.55}\rho^{-0.54}$
HYCHEM's correlation	$P_{2max} = 3.18\left(\frac{\theta Y}{\rho}\right)^{0.59} \quad (5)$	
		*for shots within the Troposphere

Table 2: Comparison of previously used approximation for P_{2max} and newly developed power correlation from HYCHEM

Similarly, to the t_{2max} correlation comparison, Northrup's approximation for P_{2max} only considers air density for shots above 4.3 km. A HYCHEM derived correlation was developed, which considers both the scaled yield and air density. Once again, this correlation can only be used at lower altitudes since low air density environments produce a single pulse. Northrup did not develop an approximation for P_{min} .

VI. HYCHEM Discussion

AIR DENSITY STUDY

In this parametric study, the thermal pulse curves for 1 kt shots were compared at various air densities. It was important to see how HYCHEM simulates the change of the double pulse as the altitude increases. It is known that, in space, nuclear detonations produce one pulse since the air density is very low, which limits any potential obstructing factors of the fireball from emitting light.

For this 1 kt and 10 kg/kt shot, it was concluded that as the air density decreased, the power curves shifted upwards. Both t_{\min} and $t_{2\max}$ appeared to be dependent on air density as well.

Lastly, the double pulses merged to form one peak at $\sim 0.005 \text{ kg/m}^3$. This is important to note as, when monitoring foreign nuclear detonations, the military uses bhangmeters to find these distinctive double pulses and calculate the yield based on t_{\min} and $t_{2\max}$. Therefore, at heights above $\sim 40 \text{ km}$, this method of monitoring nuclear detonations would not be suitable.

These predictions by HYCHEM will be validated by the film data in order to determine the validity of HYCHEM with respect to decreasing air density. Currently, most streak films are of shots with higher air densities. There is hope that the recently discovered streak films will help fill the gap in order to demonstrate how low air densities effect the shape of the double pulse at high altitudes.

MASS/YIELD STUDY

For shots within the Troposphere, it was determined the mass/yield ratio has a negligible impact on the parameters at t_{\min} and $t_{2\max}$. On the other hand, $t_{1\max}$ greatly increases with large mass/yield shots. The mass/yield ratios come into effect once the shots are within the Stratosphere. At altitudes in the lower

Stratosphere, t_{\min} and $t_{2\max}$ remain the same for each shot; however, as demonstrated in figure 19, the values of $t_{2\max}$, P_{\min} , and $P_{2\max}$ shift with each shot. The t_{\min} of the different shots appear to stay in the same vicinity despite the mass/yield ratio until t_{\min} disappears from the merging pulses.

It is interesting to note that the formation of a single pulse occurs at lower altitudes with either very small or very large mass/yield weapons – $t_{1\max}$ disappears at low mass/yields, whereas $t_{2\max}$ disappears at high mass/yields.

Once the shots reach the edge of the Stratosphere, at $\sim 50 \text{ km}$, all the different mass/yield shots produce a single light pulse.

According to this parametric study, the most discreet weapon from bhangmeters would be at higher mass/yield ratios as they only have a single pulse. In addition, the most efficient weapon would be a 100 kg/kt weapon; it has the highest peak power at high altitudes and would have enough power to affect a target at such heights. In fact, the 100 kg/kt weapon had the largest magnitude of $P_{2\max}$ even from the upper Troposphere. In addition, the 1000 kg/kt weapon had a lower peak power at 0.001 kg/m^3 than even the 1 kg/kt or 10 kg/kt shots.

Studying mass/yield effects on nuclear detonations is important in order to determine efficiency. Lower mass/yield ratio weapons are more efficient when it comes to saving resources and materials; however, as described in this study, a higher mass/yield ratio weapon, specifically a 100 kg/kt shot, has the largest potential emissive power at relatively high altitudes. Otherwise, a lower mass/yield weapon would be equally efficient for shots closer to the surface.

Fortunately, the streak films cover a variety of different types of shots: Air Drops, Tower shots, and Surface shots. These different types of shots will provide a cohort of different mass/yield ratio shots, which will enable analysis of the validity of HYCHEM's predictions.

POWER CORRELATIONS

Using the HYCHEM solutions, P_{\min} and $P_{2\max}$ correlations were developed when conducting the air density and mass/yield ratio parametric studies. It was determined that both P_{\min} and $P_{2\max}$ are dependent on the scaled yield; however, the P_{\min} curve does shift upwards as air density decreases until the shot reaches the lower Stratosphere.

At altitudes higher than ~ 11 km, the exponent of the P_{\min} curve begins to change, no longer following the simple HYCHEM correlation. For shots within the Stratosphere, neither P_{\min} nor $P_{2\max}$ can be described by simple mathematical functions.

The P_{\min} correlation is important when determining details of the thermal pulse curve of nuclear detonations and when determining the total energy emitted (i.e. integral under the curve).

These correlations and their relationships to air density and scaled yield will need to be verified using the finalized thermal power data from the streak films.

VII. Future Research

It is necessary to continue studying thermal blast as nuclear detonations are very complicated and cannot be described with simple analytical models.

In order to solve the issue regarding the POFL, the rapatronic plate data and the t_{\min} correlation (equation 2) will be used to calculate the t_{\min} of each shot. Then, the time axis will be adjusted in order for the t_{\min} of the film data to correspond to the calculated value.

In addition, the thermal power of each film needs to be finalized with validated yields. Power calculation from exposure requires the yield of the shot. At the moment, yield measurements are being completed for all shots; the yields for shots with streak films have been completed by hand and will be verified with computer-automated measurements using a second python tool by Kawahara, which measures the radius on each frame of a fireball film.

Kawahara's radius tool is not only necessary for yield measurements, but also it is necessary to determine the average surface area over time. Once all the fireball films have been analyzed, a table will be developed with the average radius of fireball over time per shot. This table can be used to calculate the surface area of a sphere via,

$$A = 4\pi r^2 \quad (6)$$

The average surface area over time is necessary in order to determine the effective surface temperature via,

$$q'' = q/A = \varepsilon\sigma(T^4 - T_0^4) \quad (7)$$

Equation (6) is only applicable for Air Drops since they have a spherical shape. Even so, Air Drops with a low height of burst develop deformities when the shockwave is reflected off the ground and protrudes the luminous hot gases of the second pulse. Therefore, even for Air Drops, the fireball shape may change over time, making equation (6) not applicable in calculating the surface temperature. In the future, when calculating the surface area of nonspherical shots, other mathematical equations need to be applied to make surface temperature calculations more accurate for all types of shots (e.g. balloon, surface, or tower) or for low height of burst shots.

HYCHEM eliminates this issue of shape deformity by assuming that the simulations have an ideally spherical shape. This is, however, not a realistic assumption as proven by the fireball films since most shots are not perfectly spherical.

Both light output and average radius measurements from the streak films and fireball films, respectively, are necessary in order to conduct an overall analysis of the reliability of HYCHEM. HYCHEM is considered as a standard simulation for nuclear physicists but has never been validated against benchmark data.

After these corrections have been completed, a direct comparison can be made to HYCHEM's prediction. Power correlations can then be developed at all three key times. In

addition, time correlations can be developed at $t_{1\max}$ and $t_{2\max}$. These correlations are very important from a military application standpoint as well as for emergency response teams, so they can appropriately allocate resources based on the peak thermal blast. The power correlations can also be applied for strike planning purposes and heat flux calculations. Finally, time correlations can be integral for future yield estimation of foreign nuclear tests.

VIII. References

[1] Taylor, G. (1950). The Formation of a Blast Wave by a Very Intense Explosion. I. Theoretical Discussion. *Proceedings of the Royal Society of London. Series A, Mathematical and Physical Sciences*, Volume 201, No. 1065, pp. 159 – 174.

[2] Northrup, J. (1996). *Handbook of Nuclear Weapon Effects: Computational Tools Abstracted from DSWA's Effects Manual One (EM-1)*. Virginia: Defense Special Weapons Agency.

[3] Cook, M. (2017). *Light Output Analysis of Nuclear Detonations*. Lawrence Livermore National Laboratory.

[4] Kawahara, A., Cook, M. (2018). *Challenges of Light Output Analysis of Nuclear Streak Films*. Lawrence Livermore National Laboratory.

IX. Acknowledgements

Dr. Gregory D. Spriggs, Jim Moye, Aaron Kawahara, Mindy Cook, Lansing Horan, Justin Nguyen, Adele Myers, Kayla Schroeder, and Trevor Pollack.